

Appendix A

Basic engineering aspects of the laminar–turbulent transition

In the previous chapters, the laminar–turbulent transition was discussed in detail as a continuous process starting from excitation of small-amplitude shear-layer disturbances up to establishment of a developed turbulent flow. Finally, we briefly comment applications of basic knowledge on instability and transition in shear flows to engineering problems of the laminar–turbulent transition prediction and control.

A.1 Transition prediction

Basically, the goal of transition prediction is to clarify whether it takes place in a flow under consideration and to find the corresponding transition Reynolds number Re_T . In early studies, the laminar–turbulent transition in boundary layers was predicted through empirical correlations between the basic flow parameters and Re_T . One of the correlations was proposed by Michel (1951) and relates the Reynolds number based on the momentum thickness Re_δ to the transition Reynolds number as

$$Re_\delta = 1.174 \left(1 + \frac{22.400}{Re_T} \right) Re_T^{0.46} .$$

This formula is applicable for attached boundary layers on airfoils with Reynolds numbers based on the wing chord length $Re_l \gtrsim 2 \times 10^6$. There exist also some correlation techniques taking into account the level of free-stream turbulence.

If the transition is modeled without resorting to empirical correlations, the most justified are the methods based on the concept of hydrodynamic stability. In this case, the prediction procedure should include three basic elements:

1. Determination of the structure of initial boundary-layer disturbances excited by external perturbations.
2. Calculation of linear development of small disturbances in the boundary layer.
3. Determination and calculation of the dominant nonlinear processes that characterize the beginning of final laminar flow breakdown.

To date certain techniques have been developed, allowing calculation of the initial amplitudes of Tollmien–Schlichting waves in some practical situations. The computations of the linear growth of boundary-layer disturbances are quite well advanced, and the adequacy of the description of Tollmien–Schlichting wave, cross-flow, and Görtler vortex amplification by the linear theory of hydrodynamic stability is confirmed experimentally. The calculation of the nonlinear stage of the transition is a more difficult problem; however, it can be sometimes bypassed in practice. Particularly, at a low free-stream turbulence level, nonlinear processes are usually very fast, and the development of small-amplitude disturbances described by the linear stability theory takes place in the major part of a transitional boundary layer. This enables the use of the linear theory for prediction of the transition ‘point,’ neglecting the details of nonlinear phenomena.

According to experimental data and estimations, the nonlinear processes usually begin to play a noticeable role at amplitudes of the Tollmien–Schlichting waves of about $u' \approx 1\%$ of external-flow velocity U_e . Since the nonlinear zone is relatively short, it is possible to admit the linear growth of disturbances in calculations a little above their real saturation amplitude and accept a transition ‘point’ at which the amplitude of a Tollmien–Schlichting wave of a certain frequency (defined during the calculations) reaches the value $u' = 2\text{--}4\%$ of U_e . The exponential growth of disturbances in the linear region makes the calculated Reynolds number insensitive to some arbitrariness in selection of the limit value Re_T . In such a way, knowing the initial amplitude and frequency characteristics of the Tollmien–Schlichting waves (from an experiment or a solution of a relevant receptivity problem), it is possible to calculate the transition position with reasonable accuracy. This idea constitutes the essence of the so-called e^N -method originally suggested by [van Ingen \(1956\)](#), [Smith and Gamberoni \(1956\)](#), which can be applied to two-dimensional boundary layers as well as to three-dimensional and separated flows dominated by convective instabilities.

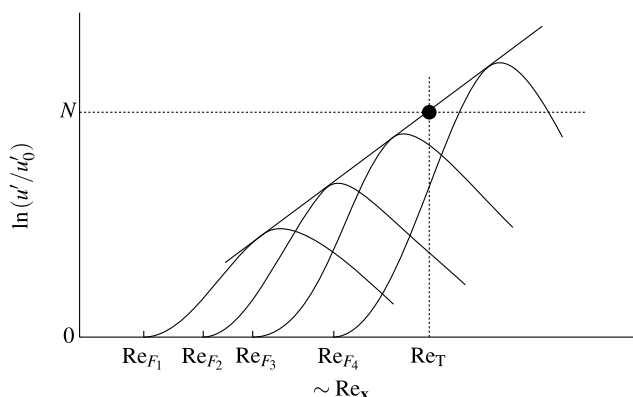


Fig. A.1 To the e^N -method: amplification curves for instability waves with different frequency parameters F

According to the method, Re_T is determined by the minimum Reynolds number at which an envelope of the growth rate curves for instability waves of different frequencies (see, Fig. A.1)

$$\ln(u'/u'_0) = - \int_{Re_F}^{Re} \alpha_i dRe_x,$$

where Re_F corresponds to branch I of the neutral stability curve for the wave with the frequency parameter F , reaches a predefined value N . Usually for plane and axisymmetric flows at a low level of free-stream turbulence, N is about 8–10.

The value of N varies depending on external-flow perturbations. For example, the results of experiments on the transition on gliders are well generalized by the e^N -method, but with the exponent $N = 15$. Such a high value of the exponent, compared with other flight experiments, is stipulated by the absence of disturbing sources, e.g., a propulsion system. The influence of free-stream turbulence, assuming its isotropy $\overline{u'^2} \approx \overline{v'^2} \approx \overline{w'^2}$, so that $Tu = \sqrt{u'^2}/U_e$, on the transition in a flat-plate boundary layer can be expressed by the interpolation formula

$$N = -8.43 - 2.4 \ln(Tu),$$

which provides acceptable accuracy in the range $Tu \approx 0.1$ –2%.

For transition prediction at a high free-stream turbulence level, methods based on consideration of spatial growth of optimal disturbances can be used. Let us assume that:

1. Initial kinetic energy of the optimal disturbances in the boundary layer is proportional to kinetic energy of isotropic disturbances of the external flow $E_e = Tu^2$ that models the receptivity of flow to external vortical perturbations;
2. Kinetic energy of the unstable disturbances is related to E_e as $E = \overline{G} Re E_e$, where \overline{G} is independent of Re , i.e., the growth is in accordance with the growth of the optimal disturbances;
3. Transition to turbulence occurs when kinetic energy of the disturbances reaches certain value $E = E_T$.

Combining these requirements yields

$$Tu \sqrt{Re_T} = K,$$

where K is a constant. Experiments testify that K is in the range of 1131–1506 at $Tu = 0.9$ –6.0.

The experimental observations of the transition in swept-wing boundary layers show the presence of quite extended regions of linear-waves development, which enables extension of the e^N -method to three-dimensional flows. The transition to turbulence in a swept-wing boundary layer can occur in the region of the negative pressure gradient as a result of crossflow instability, or downstream where there is an amplification of the Tollmien–Schlichting waves. Then it is possible to apply the e^N -method to both kinds of instability and to consider that the transition occurs if its criterion is satisfied for at least one of them. The main difficulty of application of the e^N -method for three-dimensional flows is the necessity of determining the

direction of the disturbance growth, as outlined in Sect. 6.4.2. Nevertheless, [Cebeci \(1999\)](#), [Cebeci et al \(1991\)](#) applied the procedure and showed the efficiency of the e^N -method for the ONERA–D airfoil with the angles of sweep $49\text{--}60^\circ$ and angles of attack $0\text{--}6^\circ$ at $\text{Re}_l = 1.2\text{--}1.6 \times 10^6$. [Crouch and Ng \(2000\)](#) proposed a further modification of the e^N -method to account for both the crossflow instability and the flow receptivity, which demonstrated promising results at experimental verification.

We also notice that streamwise surface curvature in the absence of centrifugal instabilities can be taken into account through local profiles of the basic flow. However, it is known that the Görtler vortices together with the Tollmien–Schlichting and crossflow waves promote an earlier transition to turbulence. Experiments on concave surfaces with domination of the Görtler vortices indicate that the transition occurs at the Görtler number based on boundary-layer momentum thickness depending on the free-stream turbulence level as

$$\text{Gö}_\delta = 9e^{-17.3\text{Tu}}.$$

Further advances in transition prediction are related to more accurate account of the nonparallel flow effects and curvature with the help of parabolized stability equations. This approach is attractive because of the low cost of the calculations comparable with the standard e^N -method. The approach also admits account of the flow receptivity in a natural manner through modification of initial and boundary conditions.

A.2 Outline of the linear control theory

The primary goal of the laminar–turbulent transition control is neutralizing disruptive shear-layer perturbations, thereby prolonging the laminar flow state. Research data on this subject are widely reported in original studies and reviewing papers while here we notice some fundamentals only.

The control strategies can be categorized based on the type of flow actuation as passive or active, depending on the absence or presence of energy consumption by the controlling device from external sources. Another classification scheme is based on the means by which the actuation changes in response to modifications in the flow. In such a way, the control strategy can be open-loop (without feedback) or closed-loop (with feedback). In open-loop control, actuator characteristics are designed in advance and remain fixed during its operation. Note that passive control is always the open-loop one.

In the control theory, the governing equations (the Navier–Stokes momentum equations and the continuity equation in our case) are called the descriptor system. In generalized form it can be written as

$$\mathcal{L} \frac{\partial \mathbf{q}}{\partial t} = \mathcal{A} \mathbf{q} + \mathcal{B} \mathbf{g} + \mathcal{D} \mathbf{w},$$

where \mathbf{q} is called the state vector consisting of disturbance velocities and pressure, \mathbf{w} is the vector of initial conditions, and \mathbf{g} is the control vector of forcing by which

the system is manipulated with the actuator described by \mathcal{B} . The sensor gives information (usually limited) about the flow state as

$$\mathbf{y} = \mathcal{C} \mathbf{q},$$

where \mathbf{y} is the vector of measured values and \mathcal{C} describes the sensor characteristics. To conduct the control in an open-loop manner, it is usually assumed that $\mathbf{y} = \mathbf{q}$ and forcing is changed through variations of actuator parameters, while the resulting measurements \mathbf{y} are monitored to reach an objective.

A closed-loop control system, in addition to the actuator and the sensor, requires a controller. To close the loop, the control system must estimate the input given by \mathbf{y} and try to tune the forcing in real time according to the measurements:

$$\mathbf{g} = \mathcal{K} \mathbf{y}$$

to reach an objective that is used to construct the feedback kernel \mathcal{K} .

It is frequently required to solve an optimization problem to design the actuator with account of given constraints, for example, to find a control technique that minimizes efforts to suppress the worst initial condition. The problem of optimization of a specified objective functional is called the optimal control problem. However, the presence of the control can make the worst initial condition different. This implies that both must be simultaneously optimized, to ensure control robustness. This approach is called the robust control.

References

- Cebeci T (1999) An engineering approach to the calculation of aerodynamic flows. Springer-Verlag, Berlin
- Cebeci T, Chen HH, Arnal D, Huang TT (1991) Three-dimensional linear stability approach to transition on wings and bodies of revolution at incidence. *AIAA J* 29(12):2077–2085
- Crouch JD, Ng LL (2000) Variable N-factor method for transition prediction in three-dimensional boundary layers. *AIAA J* 38(2):211–216
- van Ingen JL (1956) A suggested semi-empirical method for the calculation of the boundary layer transition region. VTH 74, Department of Aerospace Engineering, Delft University of Technology
- Michel R (1951) Étude de la transition sur les profils d'aile; établissement d'un critère de détermination de point de transition et calcul de la traînée de profilé incompressible. Rep. 1/1578A, Onera
- Smith AMO, Gamberoni N (1956) Transition, pressure gradient and stability theory. Rep. ES 26388, Douglas Aircraft Co., El Segundo, Cal.

Further Reading

- Abu-Ghanamm BJ, Shaw R (1980) Natural transition of boundary layers — the effects of turbulence, pressure gradient, and flow history. *J Mech Eng Sci* 22:213–228
- Airiau C, Bottaro A, Walther S, Legendre D (2003) A methodology for optimal laminar flow control: Application to the damping of Tollmien–Schlichting waves in a boundary layer. *Phys Fluids* 15(5):1131–1145
- Arnal D, Casalis G (2000) Laminar-turbulent transition prediction in three-dimensional flows. *Progr Aerosp Sci* 36:173–191
- Bewley MHTR, Henningson DS (2003) Linear feedback control and estimation of transition in plane channel flow. *J Fluid Mech* 481:149–175
- Bewley TR (2001) Flow control: New challenges for a new renaissance. *Progr Aerosp Sci* 37:21–58
- Bewley TR, Liu S (1998) Optimal and robust control and estimation of linear paths to transition. *J Fluid Mech* 365:305–349
- Bewley TR, Temam R, Ziane M (2000) A general framework for robust control in fluid mechanics. *Physica D* 138:360–392
- Cathalifaud P, Luchini P (2001) Algebraic growth in boundary layers: Optimal control by blowing and suction at the wall. *Eur J Mech B/Fluids* 19:469–490
- Collis SS, Joslin RD, Seifert A, Theofilis V (2004) Issues in active flow control: Theory, control, simulation, and experiment. *Progr Aerosp Sci* 40:237–289
- Corbett P, Bottaro A (2001) Optimal control of nonmodal disturbances in boundary layers. *Theoret Comput Fluid Dyn* 15:65–81
- van Driest ER, Blumer CB (1963) Boundary layer transition: Freestream turbulence and pressure gradient effects. *AIAA J* 1:1303–1306
- Dryden HL (1948) Recent advances in mechanics of boundary layer flow. *Adv Appl Mech* 1:1–40
- Forest AE (1977) Engineering predictions of transitional boundary-layers. CP 224, AGARD
- Henningson DS, Åkervik E (2008) The use of global modes to understand transition and perform flow control. *Phys Fluids* 20(7):031302, 1–15
- Jaffe NA, Okamura TT, Smith AMO (1970) Determination of spatial amplification factors and their application to prediction transition. *AIAA J* 8(2):301–308
- Joshi SS, Speyer JL, Kim J (1997) A systems theory approach to the feedback stabilization of infinitesimal and finite-amplitude disturbances in plane Poiseuille flow. *J Fluid Mech* 332:157–184
- Joslin RD, Gunzburger MD, Nicolaidis RA, Erlebacher G, Hussaini MY (1997) Self-contained automated methodology for optimal flow control. *AIAA J* 35(5):816–824
- Liepman HW (1945) Investigation of boundary layer transition on concave walls. *Wartime Rep. W-87, NACA*
- Mack LM (1975) A numerical method for the prediction of high speed boundary-layer transition using linear theory. *Tech. Rep. SP-347, NASA*

- Michel R, Arnal D, Coustols E (1985) Stability calculations and transition criteria on two- and three-dimensional flows. In: Kozlov VV (ed) *Laminar–Turbulent Transition*, Springer–Verlag, Berlin, IUTAM Symposium, pp 455–461
- Runiyan LJ, Gerge-Falvy D (1979) Amplification factors corresponding to transition on an unswept wing in free flight and on a swept wing in wind tunnel. AIAA Paper 79–0267
- Schmid PJ, Henningson DS (1994) Optimal energy density growth in Hagen–Poiseuille flow. *J Fluid Mech* 277:197–225
- Walther S, Airiau C, Bottaro A (2001) Optimal control of Tollmien–Schlichting waves in a developing boundary layer. *Phys Fluids* 13(7):2087–2096
- White FM (1974) *Viscous fluid flow*. McGraw-Hill, New York

Index

A

adjoint pressure, 25
adjoint stress, 182
adjoint velocity, 25
algorithm
 Arnoldi, 44
 QZ, 42, 44
amplification rate, *see* growth rate
attraction radius, 5
attractor, 4

B

bi-orthogonality condition, 26
bifurcation, 4
boundary conditions, *see* conditions, boundary
boundary layer, 21, 24, 30
 asymptotic-suction, 14, 115
 attached, 21, 133, 259
 axisymmetric, 91
 Blasius, 7, 9, 20, 47–50, 53, 55, 60, 85, 132
 curved-wall, 67
 reattached, 130, 132
 self-similar, 51, 60, 67, 71, 109, 114
 swept-wing, 108, 109, 137, 156, 209, 225, 261
 variable-viscosity, 112
boundary-layer equations, *see* equations, Prandtl
burst, turbulent, 243–246

C

Chebyshev polynomial, 41
circular frequency, *see* frequency, circular
collocation point, 40, 97

Gauss–Lobatto, 41
trigonometric, 104
concomitant, bilinear, 25, 192
conditions, boundary, 5, 9, 13, 19, 27, 28, 41, 68, 69, 71, 74–76, 80, 91, 93, 98, 114, 180, 184, 192, 262
 asymptotic, 53
 constant, 3
 Dirichlet, 41, 94, 99
 homogeneous, 16, 17, 24, 25, 29, 53, 57, 94–96, 98, 104, 106, 122, 164, 166, 167, 208, 211
 inhomogeneous, 179, 182
 linearized, 183
 natural, 9
 Neumann, 41
 no-slip, 14, 26, 28, 29, 52, 93, 112, 117
 periodic, 102, 104
 viscous, 21
conditions, initial, 5, 13, 14, 79, 80, 98, 111, 149, 160, 161, 163, 167, 168, 223, 229, 262
control
 active, 262
 closed-loop, 262
 open-loop, 262
 optimal, 263
 passive, 262
 robust, 162, 263
coordinate system
 Cartesian, 10, 13, 16, 25, 91, 94, 115, 151
 cylindrical, 13, 67, 72, 91
 local, 108
 model-fitted, 69, 108
 natural, *see* coordinate system, model-fitted
 Squire transformation, 111, 160
 Stuart transformation, 160

wavevector-aligned, 111, 160
 criterion
 circulation, 71, 73, 76
 inflection point, 19, 52, 107, 111
 maximum vorticity, 19
 critical layer, *see* layer, critical
 crossflow, 109–111, 137, 139, 207, 209, 225

D

deformation tensor, 10
 dispersion, 16, 17, 23, 111, 135, 136, 153, 156, 160, 228, 230
 displacement thickness, 47, 79, 119, 191
 disturbance
 asymptotic behavior of, 4, 150, 159
 convective, 5
 finite, 7, 8, 230
 free-stream, 30
 fundamental, 230
 infinitesimal, 7, 8, 14
 initial, 7, 167, 181, 247
 localized, 150, 171, 195
 modal, 13
 neutral, 8
 optimal, 162, 164, 166–168, 173, 214, 261
 primary, 207, 209
 secondary, 207, 209, 215
 small, 17, 21, 39, 47, 57, 109, 115, 121, 135, 136, 149, 171, 229, 259, 260
 symmetric, 96
 three-dimensional, 15
 transient, 24, 36, 161, 171
 two-dimensional, 15
 disturbance energy, 10, 21, 36, 59, 60, 116, 150, 159–161, 167, 171, 209, 235, 261
 disturbance kinetic energy, *see* disturbance energy
 disturbance profile
 amplitude, 15
 phase, 15

E

e^N -method, 260
 eigenfunctions, 16, 17, 24, 30, 37, 93, 106, 161
 adjoint, 154, 182, 193
 complete set of, 27
 even, 37
 generalized, 27
 odd, 37
 orthogonal, 24
 eigenvalue, 17, 21, 24
 leading, 37, 43, 44, 49, 105, 106, 167

 secondary, 208
 spatial, 22
 temporal, 38
 eigenvalue problem, 16–18, 22, 76, 81, 93, 96, 99, 100, 106, 122, 164, 177, 208
 generalized, 44
 nonlinear, 43, 86
 solution, numerical, 42
 equation
 Blasius, 52
 continuity, 10, 13, 14, 25, 50, 67, 80, 91, 98, 99, 111, 207, 262
 energy balance, *see* equation, Reynolds–Orr
 Falkner–Skan, 51
 Falkner–Skan–Cooke, 109
 Landau, 8
 normal vorticity, *see* equation, Squire
 Orr–Sommerfeld, 16, 18, 20, 23, 35, 37, 41, 51, 75, 77, 81, 86, 110, 121, 154, 208
 Orr–Sommerfeld, adjoint, 26
 Orr–Sommerfeld, asymptotic behavior of, 27
 Poisson, 15, 94, 97, 98, 102
 Rayleigh, 19, 171
 Reynolds–Orr, 10
 Squire, 17, 35, 37, 110
 Voigt, 116
 equations
 Navier–Stokes, 4, 9, 55, 58, 67, 69, 92, 98, 181, 223, 262
 Navier–Stokes, adjoint, 25
 Navier–Stokes, linearized, 25, 57, 58, 67, 92, 113, 117, 119, 159, 160, 164, 179, 182, 183, 194, 207
 Dean, 77
 Görtler, 81
 Görtler, adjoint, 192, 193
 Navier, 115
 Prandtl, 70, 107, 109, 114
 Taylor, 75
 excitation
 hard, 8, 9
 soft, 8
 excitation, efficiency of, 182
 experimental modeling, *see* simulation, experimental

F

flapping, 130, 139
 Floquet parameter, 105
 Floquet theory, 102, 105, 208
 Fredholm alternative, 57

free-stream turbulence, 49, 51, 177, 189, 197, 212, 253, 259, 261, 262
 high, 168, 195, 197, 231, 235, 252, 261
 low, 224, 225, 233, 252, 260, 261
 suppression, 60
 frequency parameter, 47, 61, 81, 83, 86
 frequency, circular, 15

G

growth
 exponential, 134, 136, 212
 superexponential, 228
 transient, 4, 7, 10, 160, 161, 164
 growth rate, 10, 15, 19, 22, 38, 40, 55, 57, 59, 63, 75, 80, 81, 83, 86, 134–138, 149, 150, 156, 160, 161, 167, 230, 235, 252
 maximum, 17, 137, 153
 reduced, 16
 reduction of, 114, 120
 spatial, 23, 133, 138, 155
 spatial-to-temporal transformation of, 23
 temporal, 23

H

Hilbert space, 26
 hot-wire anemometer, 40, 49, 60, 78, 131, 139, 155, 186, 225, 243, 244, 250

I

impulse response, 21
 increment, *see* growth rate
 inflection point, 19, 21, 37, 107, 113, 114, 132–134, 137
 initial conditions, *see* conditions
 instability
 absolute, 4, 5, 37, 151, 153, 154, 208, 215, 253
 absolute, centrifugal, 72
 algebraic, 30, 159, 161
 compliance-induced, 120
 convective, 4, 22, 111, 130, 137, 151, 153, 154, 177, 189, 208, 253
 convective, centrifugal, 72, 77, 78
 crossflow, 111, 114, 139, 153, 156, 177, 180, 181, 190, 194, 209, 212, 214, 260–262
 Dean, 72, 209
 Eckhaus, 210
 global, 94, 130, 253
 Görtler, 72, 78, 79, 83, 177, 192, 209, 214, 260, 262
 inviscid, 19, 36, 73, 111, 113

secondary, 102
 Taylor, 72, 209
 Tollmien–Schlichting, 18, 38, 43, 44, 49, 50, 72, 107, 114, 132, 150, 153, 170, 171, 177, 179, 185, 186, 207, 208, 223, 225, 232, 233, 235, 243, 260, 262
 viscous, 20, 85, 107, 185
 interaction, viscous-inviscid, 139
 intermittency, 243
 interpolation points, *see* collocation point

J

Jacobian, 103

K

knot, *see* collocation point
 Kronecker tensor product, *see* tensor product

L

Lagrange identity, 25, 26, 182, 192
 Λ -structure, 215, 225, 227
 Λ -vortex, *see* Λ -structure
 layer, critical, 19, 213, 223

M

metastability, 8, 9, 39
 mode
 detuned, 106
 mixed, *see* mode, detuned
 normal, 15, 18, 21, 24, 26, 37, 49, 76, 96, 106, 160, 163, 182, 185, 187, 210
 sinuous, 106, 211, 212, 214
 spurious, 41, 98
 varicose, 106, 211, 212, 214
 modulus
 bulk, 116
 shear, 116
 momentum thickness, 114, 132, 134, 259, 262

N

narrow-gap approximation, 68, 69
 near-wall jet, 52
 node, *see* collocation point
 number
 Dean, 77, 78
 Görtler, 7, 79, 194
 critical, 7
 subcritical, 81
 transition, 7
 Reynolds, 6
 critical, 6, 37, 47, 51, 94, 96, 102, 113, 115, 120, 153, 186

- subcritical, 10, 161, 164, 172, 186, 214, 229
 - transition, 7, 39, 243, 245, 246, 259, 260
 - Taylor, 75
- P**
- parametric resonance, *see* resonance, parametric
 - particle image velocimetry, 139
 - Poisson's ratio, 116
 - pressure gradient
 - favorable, 107
 - unfavorable, 107
 - pressure gradient parameter, 52, 109
 - principle of exchange of stabilities, *see* stabilities, exchange of
 - problem
 - adjoint, 24, 167, 184, 192
 - boundary-value, 4
 - initial-value, 4, 24
- Q**
- QR-decomposition, 100
 - QZ-algorithm, *see* algorithm, QZ
- R**
- radius, nodal, 73
 - Rayleigh line, 73
 - Rayleigh quotient, 10, 163
 - Rayleigh theorem
 - first, *see* criterion, inflection point
 - second, 19
 - receptivity function, 180, 182, 184, 188, 191, 194
 - resonance, 178, 209
 - resonance, parametric, 227, 229, 231
 - root-mean-square amplitude, 39, 59
- S**
- semicircle theorem, 19
 - shape factor, 134
 - shedding, *see* vortex shedding
 - simulation
 - direct numerical, 55, 58, 60, 133, 181, 228
 - experimental, 63, 184, 244
 - solvability condition, *see* Fredholm alternative
 - source
 - far-field, 85, 150, 159, 177
 - near-field, 150, 159, 161, 177
 - spectrum
 - continuous, 27–30, 53, 161, 162
 - discrete, 27, 28, 30, 229
 - spike, 225, 227, 243
 - spline, cubic, 139
 - spot
 - turbulent, 170, 224, 232, 235, 243, 245
 - turbulent, incipient, 232, 233, 249
 - stabilities, exchange of, 5, 7, 8, 75, 77, 78
 - stability
 - asymptotic, 5, 13
 - conditional, 5, 36
 - global, 5, 7
 - indefinite, *see* stability, neutral
 - linear, 13
 - local approach, *see* stability, linear
 - locally-parallel approach
 - locally-parallel approach, 14, 81, 133, 139, 191, 194, 210
 - quasi-parallel approach, *see* stability, linear locally-parallel approach
 - monotonic, 5, 36, 161
 - neutral, 3, 17, 19
 - asymptotic, 20, 50, 81
 - curve of, 20, 22, 24, 37, 39, 47, 48, 50, 58, 60, 62, 63, 73, 81–83, 86, 113, 114, 153, 234
 - surface of, 17, 18, 22, 24, 86
 - parallel approach, 13
 - streak, *see* streaky structure
 - streaky structure, 164, 168, 170, 171, 194, 195, 197, 209, 213–215, 229, 232, 252
- T**
- tensor product, 97
 - transition scenario, 154, 162, 177, 233
 - transpose, 14
 - Hermitian, 100
 - turbulent burst, *see* burst, turbulent
- V**
- velocity
 - group, 21, 23, 111, 151, 153, 170, 215
 - phase, 15, 19, 22, 29, 85, 132, 135, 155, 207, 215, 234
 - vibrating-ribbon technique, 49, 61, 149, 188, 227, 235
 - viscosity
 - dynamic, 6, 112, 123
 - kinematic, 6, 79, 113, 121, 123
 - second, 116
 - Voigt model, *see* equation, Voigt
 - vortex shedding, 130

vortex, coherent, 231

W

wave

- two-dimensional, 24
- axisymmetric, 72, 73, 75, 94, 136
- dilatation, 116
- equivoluminal, 116
- helical, 72, 76, 136
- oblique, 13, 15, 24, 30, 55, 85, 119, 135, 136, 156, 166, 168, 170, 216, 225, 228
- plane, 15
- pressure, 28
- primary, 208, 243

Rayleigh, 19

subharmonic, 208, 230, 243

two-dimensional, 15, 19, 24, 135, 136, 207, 225, 228

vorticity, 17, 18, 29, 30

wave train, 149, 150, 155

wavelength parameter, 81

wavenumber

- azimuthal, 76, 92

- streamwise, 15

- transverse, 15

wavevector, 15, 22, 153, 156, 160, 228

- angle, 15, 107, 136

- magnitude, 24